



Femtoscopic measurements in p +Pb collisions at $\sqrt{s_{\text{NN}}} = 5.02$ TeV with ATLAS at the LHC

Markus K. Köhler
(on behalf of the ATLAS Collaboration)¹

Weizmann Institute of Science, Israel

Abstract

Recent measurements in two-particle correlations in p +Pb collisions suggest collective behavior reminiscent of that observed in Pb+Pb. Femtoscopic measurements may provide useful insight on this behavior because they image the spatio-temporal size of the particle emitting region. This proceeding presents identical-pion Hanbury Brown and Twiss (HBT) measurements from ATLAS using one- and three-dimensional correlation functions. Pions are identified using dE/dx measured in the pixel detector. Correlation functions and the resulting HBT radii are shown as a function of pair momentum (k_T) and collision centrality.

Keywords: ATLAS, p +Pb collisions, Femtoscopia

1. Introduction

Long range two-particle correlation functions in relative pseudorapidity and relative azimuthal angle in pp and p +Pb collisions measured at the LHC are consistent with a possible collective behaviour [1, 2, 3], reminiscent to that observed in Pb+Pb collisions, see e.g. [4].

Femtoscopic measurements in pp and p +Pb collisions [5, 6] allow the investigation of the time evolution of small colliding systems. This proceeding reports the first measurement of the centrality and momentum dependence of same- and opposite-sign pion pair correlations in p +Pb collisions at $\sqrt{s_{\text{NN}}} = 5.02$ TeV measured by the ATLAS experiment.

2. Data analysis

This analysis uses a data sample with an integrated luminosity of 28.1 nb^{-1} of p +Pb collisions, measured in 2013 by the ATLAS detector [7]. The Pb beam had an energy of 1.57 TeV per nucleon and the opposing p beam had an energy 4 TeV, resulting in a center of mass energy of $\sqrt{s_{\text{NN}}} = 5.02$ TeV. The centrality is determined using the total transverse energy measured in the forward calorimeter on the Pb-going side, see e.g. Ref. [8] for more information.

¹A list of members of the ATLAS Collaboration and acknowledgements can be found at the end of this issue.

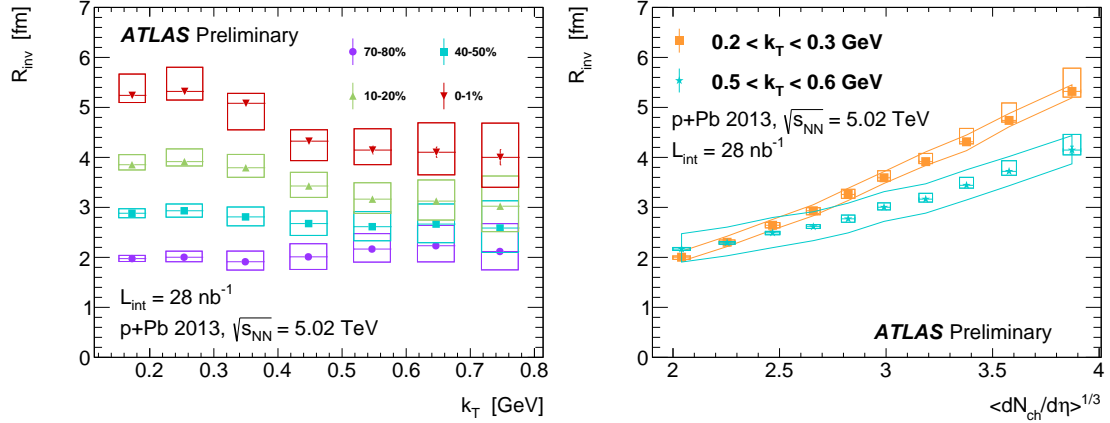


Fig. 1. Invariant radii R_{inv} as a function of k_T in different centrality bins (left panel) and as a function of the cube root of the average charged particle multiplicity, $\langle dN_{ch}/d\eta \rangle^{1/3}$, in two k_T intercepts (right panel). Figures from [9].

Reconstructed tracks are required to have a transverse momentum $p_T > 0.1$ GeV and to be within the pseudorapidity² range $|\eta| < 2.5$. Pions are identified using the dE/dx information from the silicon pixel detector. Pion pairs are required to have $|\Delta\phi| < \pi/2$ and to be within the pair rapidity region of $|\eta_k| < 1.5$. Opposite-sign pairs that have an invariant mass close to the masses of ρ^0 , K_S^0 and ϕ are rejected.

The two-particle correlation function is defined as $C(q) = A(q)/B(q)$, where q is the relative momentum $q = p^a - p^b$, $A(q) = dN/dq|_{\text{same}}$ is the same-event distribution and $B(q) = dN/dq|_{\text{mixed}}$ is the mixed-event distribution in the same event class.

In three dimensions, a longitudinally co-moving frame is chosen, such that $p_z^a = -p_z^b$. The coordinates are defined in the Bertsch-Pratt convention [10, 11], where q_{out} shows in the direction of the pair momentum, q_{long} shows in the direction of the beam and q_{side} is perpendicular to the q_{out} and q_{long} . A graphical visualization of Bertsch-Pratt coordinates is shown e.g. in Ref. [12]. Using the Bowler-Sinyukow [13, 14] parametrization, the correlation function can be written as

$$C(q) = [(1 - \lambda) + \lambda K(q) C_{BE}(q)] \Omega(q), \quad (1)$$

where λ , $K(q)$, $C_{BE}(q)$ and $\Omega(q)$ is the correlation strength, a correction factor for final-state interactions, the Bose-Einstein enhancement factor and the contribution from non-femtoscopic correlations, respectively. The Bose-Einstein factor $C_{BE}(q)$ in the correlation function is fit to an exponential function

$$C_{BE}(q) = 1 + \exp(-\hat{R}\hat{q}), \quad (2)$$

where \hat{R} and \hat{q} are the invariant radius R_{inv} and the invariant momentum q_{inv} in the one-dimensional case and a diagonal matrix with the entries $\mathcal{R} = \text{diag}(R_{out}, R_{long}, R_{side})$ and $\vec{q} = (q_{out}, q_{long}, q_{side})$ in the three-dimensional case, respectively.

The non-femtoscopic contribution to the correlation function $\Omega(q)$ is estimated by a fit to the opposite-sign pair distribution

$$\Omega(q_{inv}) = \mathcal{N} \left[1 + \lambda_{bkg} \exp(-|R_{bkg} q_{inv}|^{\alpha_{bkg}}) \right], \quad (3)$$

where \mathcal{N} is an arbitrary normalization factor, λ_{bkg} is the experimental correlation strength, R_{bkg} is a parameter for the width and α_{bkg} is a shape parameter. The origin of this background is identified to be from hard

²ATLAS uses a right-handed coordinate system with its origin at the nominal interaction point (IP) in the centre of the detector and the z -axis along the beam pipe. The x -axis points from the IP to the centre of the LHC ring, and the y -axis points upward. Cylindrical coordinates (r, ϕ) are used in the transverse plane, ϕ being the azimuthal angle around the z -axis. The pseudorapidity is defined in terms of the polar angle θ as $\eta = -\ln(\theta/2)$.

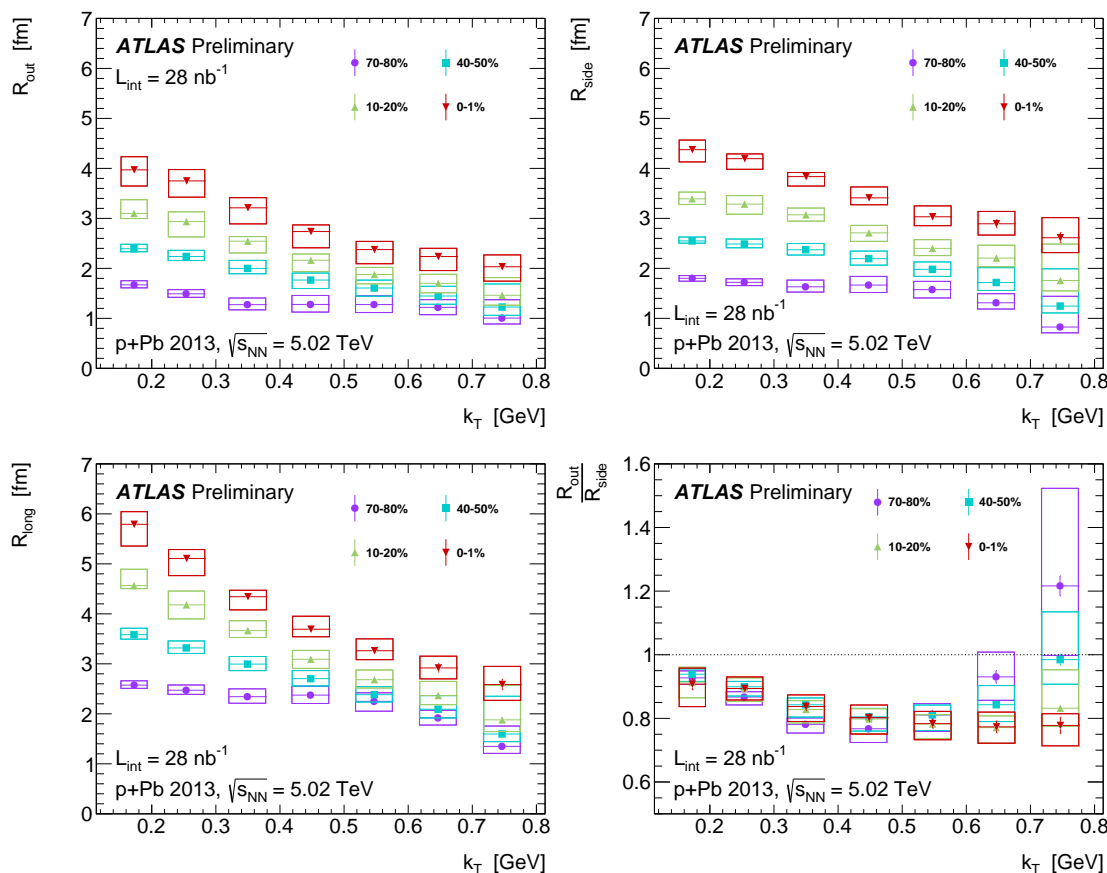


Fig. 2. The radii R_{out} (upper left panel), R_{side} (upper right panel) and R_{long} (lower left panel) as a function of k_T in different centrality bins. The lower right panel shows the ratio of R_{out}/R_{side} as function of k_T . Figures from [9].

processes, such as particles from jet fragmentation. A mapping of the parameters λ_{bkg} and R_{bkg} between opposite-sign and same-sign is extracted from Monte Carlo simulations. It should be noted, that all parameters describing the background are constrained by this method. Systematic uncertainties are estimated by taking into account the hard process background description, particle identification, effective Coulomb correction size R_{eff} , charge asymmetry, and two particle effects. More details on the data analysis procedure can be found in Ref. [9].

3. Results and conclusions

Figure 1 shows the invariant radii R_{inv} as a function of the pair momentum k_T and as a function of cube root of the average charged particle multiplicity $\langle dN_{ch}/d\eta \rangle^{1/3}$. The measured radii are observed to decrease with increasing k_T , which is consistent with collective expansion. This behavior is less severe for peripheral collisions.

Figure 2 shows the results for the radii R_{out} , R_{long} and R_{side} and the ratio R_{out}/R_{side} as a function of the pair momentum k_T for different centralities. The radii show a decreasing trend with increasing k_T . In the most central events 0 – 1 %, the radii are about a factor 2.5 larger than in peripheral collisions 70 – 80 %. The ratio R_{out}/R_{side} falls significantly below 1, indicating a very rapid and explosive expansion of the fireball. This behavior can be explained by a combination of pre-thermalized acceleration, a stiffer equation of state, and adding viscous corrections [15].

In Fig. 3, the product $R_{out}R_{side}R_{long}$, which scales linearly with the volume, is shown as a function of the

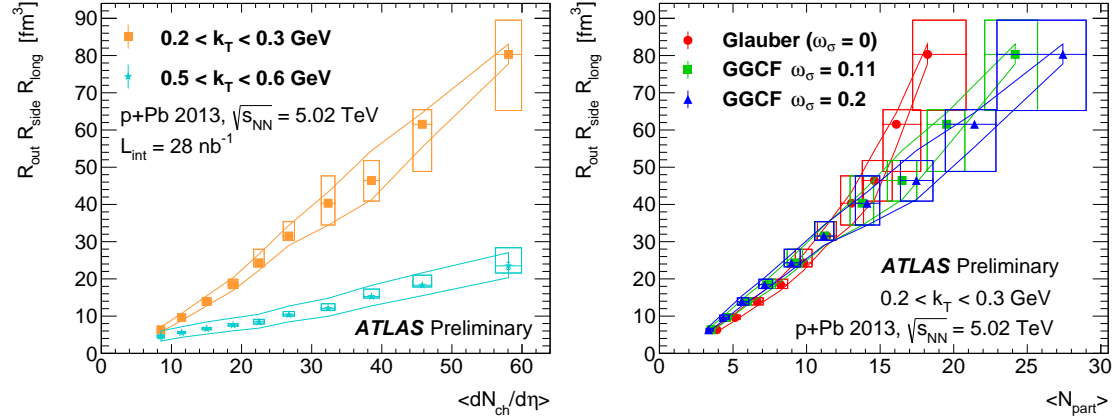


Fig. 3. The product $R_{out}R_{side}R_{long}$ as a function of $\langle dN_{ch}/d\eta \rangle$ for two different k_T intervals (left panel) and as a function of $\langle N_{part} \rangle$ for three different models describing the initial geometry. Figures from [9].

average multiplicity $\langle dN_{ch}/d\eta \rangle$ for two intercepts of the pair momentum in the left panel. The volume is linearly increasing with increasing $\langle dN_{ch}/d\eta \rangle$, indicating a constant source density at the moment of freeze-out. The product is also shown as a function of $\langle N_{part} \rangle$ for the Glauber Model and for the Glauber-Gribov Color Fluctuation model (GGCF), including different values ω_σ for the magnitude of the color fluctuations. The extraction of centrality dependent values of $\langle N_{part} \rangle$ is described in Ref. [8].

4. Acknowledgement

This work was supported by U.S. Department of Energy grant DE-FG02-86ER40281.

References

- [1] CMS Collaboration, JHEP 09 (2010) 091
- [2] CMS Collaboration, Phys. Lett. B718 (2013) 795
- [3] ATLAS Collaboration, submitted to Phys. Rev. Lett., Preprint arXiv:1509.04776 [hep-ex]
- [4] K. Aamodt *et al.*, ALICE Collaboration, Phys. Lett. B696 (2011) 328
- [5] ATLAS Collaboration, Eur. Phys. J. C75 (2015) 466
- [6] J. Adam *et al.*, ALICE Collaboration, Phys. Rev. C91 (2015) 034906
- [7] ATLAS Collaboration, JINST 3 (2008) S08003
- [8] ATLAS Collaboration, submitted to EPJC, Preprint arXiv:1508.00848 [hep-ex]
- [9] ATLAS Collaboration, ATLAS-CONF-2015-054 (2015), URL:<http://cds.cern.ch/record/2055675/>
- [10] G. F. Bertsch, Nucl. Phys. A498 (1989) 173
- [11] S. Pratt, Phys. Rev. D33 (1986) 1314
- [12] M. Lisa, S. Pratt, R. Scholz and U. Wiedemann, Ann. Rev. Nucl. Part. Sci. 55, (2005) 357
- [13] M. Bowler, Phys. Lett. B270 (1991) 69
- [14] Y. Sinyukow, Phys. Lett. B432 (1998) 248
- [15] S. Pratt, Phys. Rev. Lett. 102 (2009) 232301